



HAL
open science

Détection de l'amorçage de fissure dans les matériaux quasi-fragiles par corrélation d'images numériques

Raja Romani, Dominique Leguillon, Karam Sab, Robert Le Roy, Michel Bornert

► **To cite this version:**

Raja Romani, Dominique Leguillon, Karam Sab, Robert Le Roy, Michel Bornert. Détection de l'amorçage de fissure dans les matériaux quasi-fragiles par corrélation d'images numériques. CFM 2013 - 21ème Congrès Français de Mécanique, Aug 2013, Bordeaux, France. hal-03439971

HAL Id: hal-03439971

<https://hal.science/hal-03439971>

Submitted on 22 Nov 2021

HAL is a multi-disciplinary open access archive for the deposit and dissemination of scientific research documents, whether they are published or not. The documents may come from teaching and research institutions in France or abroad, or from public or private research centers.

L'archive ouverte pluridisciplinaire **HAL**, est destinée au dépôt et à la diffusion de documents scientifiques de niveau recherche, publiés ou non, émanant des établissements d'enseignement et de recherche français ou étrangers, des laboratoires publics ou privés.

Identification and validation of crack onset criterion by digital image correlation in quasi-brittle materials under compression

R. ROMANI^a, M. BORNERT^b, D. LEGUILLON^a, R. LEROY^{b,c}, K. SAB^b

a. Institut Jean Le Rond d'Alembert, CNRS, Université P. et M. Curie, 4 place Jussieu 75005 PARIS

b. Université Paris-Est, Laboratoire Navier, CNRS, ENPC, IFSTTAR, F-77455 Marne-la-Vallée

c. Ecole Nationale Supérieure d'Architecture Paris-Malaquais (ENSAPM), 14 rue Bonaparte 75272 Paris

Résumé :

Les géomatériaux présentent une meilleure résistance à rupture en compression qu'en traction. La présence de cavités dans ceux-ci limite cette propriété. Dans ce travail, on s'intéresse à la première étape du processus de rupture : l'amorçage de fissures, qui est analysé sur un matériau modèle, le plâtre. L'amorçage est étudié sur une éprouvette rectangulaire présentant une cavité cylindrique, soumise à un chargement de compression. L'étude comporte une partie expérimentale et une partie théorique. La théorie est basée sur l'utilisation du critère mixte de Leguillon, la partie expérimentale inclut d'une part la détermination des propriétés mécaniques du plâtre et d'autre part les essais de compression. L'amorçage expérimental, difficilement détectable à l'oeil, est déterminé par corrélation d'images numériques grâce à un critère objectif sur l'évolution du champ de déformation mesuré. Les résultats expérimentaux sont confrontés avec succès aux résultats théoriques.

Abstract:

Geomaterials exhibit better resistance to rupture in compression than in tension. The presence of cavities in these materials limits this property. In this work, we focus on the first stage of the rupture process: crack initiation, which is investigated in plaster, considered as a model material. The crack onset is studied in a rectangular specimen with a cylindrical cavity, loaded in compression. The study includes an experimental part and a theoretical part: the theory is based on the use of Leguillon's mixed criterion, and the experimental part includes the determination of the mechanical properties of plaster and the compression tests. Due to the difficulty of the detection of the crack initiation by the naked eye, the technique of Digital Image Correlation is used to identify the crack onset with an objective criterion on the evolution of the strain field measured. The experimental results are in agreement with the theoretical results.

Mots clefs: elasticity, fracture mechanics, compression, crack onset, mixed criterion, Digital Image Correlation, ...

1 Introduction

Geomaterials such as concrete, plaster or rocks are heterogeneous and quasi-brittle materials containing pores. Under a tension load, the crack initiates from the inhomogeneity and then propagates unstably causing the rupture of the structure. In civil engineering and rock mechanics, compressive loading is more often met than tension. Under compression, a tension crack initiates from the inhomogeneity in the direction of the load [1]. This crack is stable: the crack propagates with increasing load and doesn't cause immediately the rupture of the whole structure.

The purpose of this paper is to study the crack initiation in quasi-brittle materials under compressive loading. The plaster is chosen as a model material and its mechanical properties are determined in a first step. Next, compression tests are realized on drilled specimens. As the initiation of crack cannot be detected with the naked eye, Digital Image Correlation (DIC) [2] is used to determine the crack onset experimentally.

Leguillon's mixed criterion [3] offered a theoretical prediction of crack initiation. The criterion is based on two conditions relying on energy and stress. Neither one nor the other is sufficient, their combination leads to satisfying prediction in various other situations [4].

2 Mechanical properties of plaster

A powder plaster of the Lafarge company named Prestia Profilia 35® is used because of its short hardening time. The preparation of the plaster specimens goes through the following steps: preparing the mass of water and the mass of plaster satisfying the volume of the mould and a mixing ratio equal to 0.33. In the mixer, the water is poured first and then the plaster is added. Mixing is done for one minute at a very low speed (65rpm) to avoid the formation of air bubbles. The mixture is then poured into the appropriate mould and left at room temperature for 72h in order to be dry enough to carry out tests.

2.1 Young's modulus E

Two strain gauges are mounted on the two faces of the sample with dimensions 100mm x 65mm x 20mm loaded under compression in order to measure the lateral and axial deformation during loading.

Compressing machine allows recording the force applied and the local deformation of the gauge in the direction of loading. Young's modulus is then calculated taking the slope of the stress/strain curve. Taking the average of the two modules measured on the two sides of the specimen gives $E=13,5\text{GPa}$.

Before mounting the gauges on the sample, a speckle of black paint is applied on the specimen. A camera films the sample during the compression test. The images of the test are then treated by DIC. The technique allows determining in each image, the deformation of the specimen. Young's modulus is determined by taking the slope of the curve stress (given by the machine) strain in the direction of the load (determined by DIC). The Young modulus found by DIC is $E=12\text{GPa}$ in agreement with the one given using gauges. Hereinafter E is taken equal to 12GPa.

2.2 Tensile strength σ_c

Three point bending test on an unnotched sample of dimensions 160mm x 40mm x 40mm is used to measure the tensile strength (Figure 1.a).

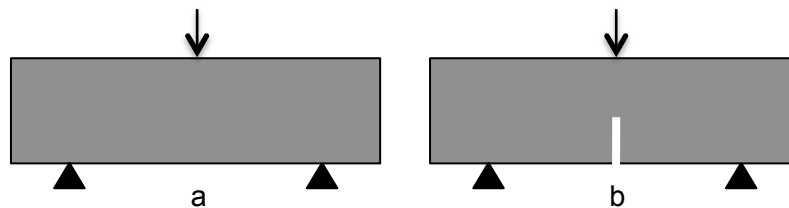


FIG. 1 – Three point bending test on unnotched sample (a) and notched sample (b)

In three point bending test, failure occurs in mode I. A crack initiates at the centre of the lower edge of the sample. This crack is unstable and leads rapidly to the failure of the whole specimen. The tensile strength corresponds to the maximum tension reached in the centre of the lower edge of the sample before failure. To determine it, a 2D Finite Element computation is used to model the test: A displacement equal to the average displacement at rupture retrieved from experiments is imposed in the model. For a Young modulus of 12GPa chosen for the structure and a Poisson ratio equal to 0.3 [5], the tensile strength is $\sigma_c=10\text{MPa}$.

2.3 Toughness G_c

Toughness measurements are made on pre-cracked samples of the same dimensions as those used to determine the tensile strength (Figure 1.b). The slit in the sample is obtained by gluing a metallic lamella in the mould before casting plaster. The experimental bending test allows identifying the average displacement at rupture of the sample. For this displacement, the critical stress intensity factor K_{Ic} at the tip of the crack is determined by contour integrals surrounding the crack tip and connecting the two edges of the crack [6]. The Irwin relation can then convert K_{Ic} to G_c :

$$G_c = \frac{1-\nu^2}{E} K_{Ic}^2 \quad (1)$$

The value of G_c found is then corrected taking into account the notch-root radius, which is the width of the pre-existing crack [7]. The toughness obtained is $G_c = 4.2 \text{ J/m}^2$.

3 Crack onset in plaster

3.1 Experimental procedure

The dimensions of the drilled samples are 100mm x 65mm x 20mm. The diameters of holes are: 3, 4, 5 and 6 mm. Compression load is applied continuously at a strain rate of 0.2mm/min. To avoid friction at the contact between the two plateaus of the compression machine and the surface of the sample, PMMA plates are placed on the top and bottom of the plaster specimen. A camera (Baumer HXC20, CMOS sensor with 2048x1088 pixels, equipped with a ZEISS Makro-Planar 100mm macro lens) is used to acquire images of the samples during the compression test, at a 20Hz frame rate.

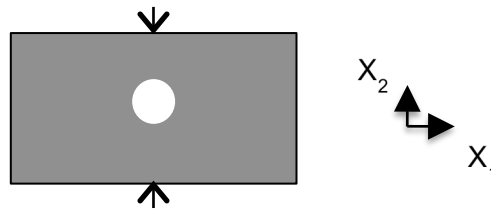


FIG. 2– Compression test on drilled sample

The rupture of the whole specimen occurs without seeing any tension crack arising or growing from the hole in the loading direction. In order to identify the crack onset, 2D-DIC is used. The technique requires the preparation of the sample with a random distribution of grey levels obtained by applying a speckle of black paint on the specimen of appropriate size. A light system is used to lighten the surface of the sample. The area of interest filmed during the test is a surface of 18 mm x 10 mm centred on the cavity. The in-house CMV software is used for the DIC analysis. The DIC provides the strain field in each image taken during the test [8]. Once the deformations are known, a map of the 11-component of the strain field is drawn in each image. They show two red areas corresponding to the two cracks, which take place in the north and south poles of the cavity in the direction of the compression load (Figure 3).

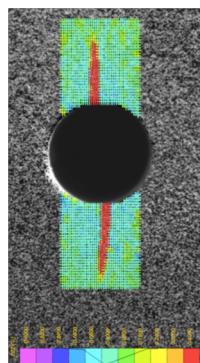


FIG. 3– Detection of cracks by DIC

The diameter of the cavity in Figure 4 is 5 mm. As already mentioned, it is impossible to detect the crack onset from the naked eye and even quite difficult directly from the treated images. In order to detect the nucleation, the history of the 11-component of the strain field is followed on points located on two lines (blue lines in Figure 4): one orthogonal to the expected crack path emanating from the north pole and close to the top of the cavity and the other orthogonal to the crack path emanating from the south pole and close to the bottom of the cavity.

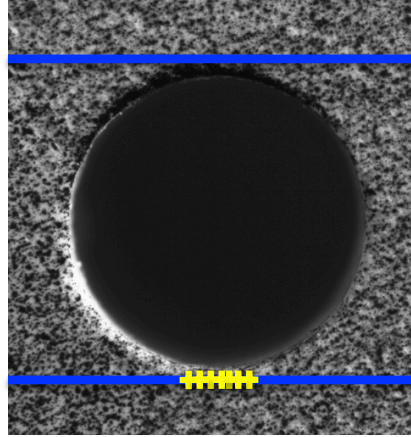


FIG. 4– Location of the points used to follow the history of strain in order to detect the crack onset

Figure 5 shows the evolution of the local strain ε_{11} at 7 points (yellow points in Figure 4) on the line located at the bottom of the hole.

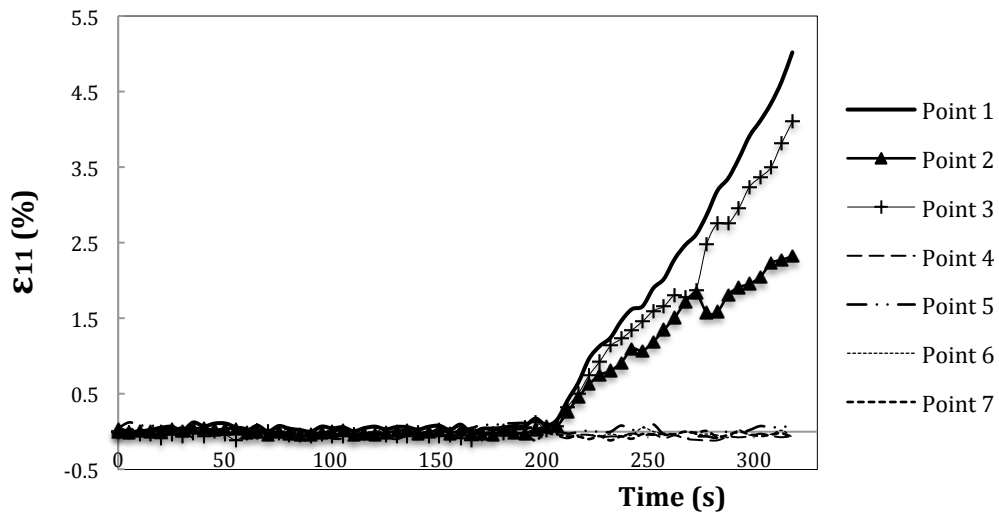


FIG. 5– History of the strain ε_{11} at 7 points at the bottom of the hole. Method to detect the crack onset

The strain ε_{11} remains small for points away of the crack. For the points assumed close to the crack, ε_{11} is small at first and then increases at a given time corresponding to a given load. We suppose that nucleation occurs at the point where these curves merge ($t = 210$ s on Figure 5), which can unambiguously be determined.

3.2 Mixed criterion

In brittle fracture mechanics, two criteria are often used: the maximum stress criterion and the Griffith criterion. The former predicts the ruin of the structure in tension if a local tensile stress reaches the tensile strength of the material σ_c . The latter states that failure occurs if the energy release rate is larger than the material toughness.

In the mixed criterion, these two conditions are assumed to be necessary but neither one nor the other is sufficient. The verification of both these criteria allows determining crack initiation [3].

$$\sigma(l) \geq \sigma_c \text{ and } G(l) \geq G_c \quad (2)$$

where σ , σ_c , G , G_c and l are respectively the local tensile stress, the tensile strength, the incremental energy release rate, the toughness of the material and the crack length.

The diameter of the cavity, d (3, 4, 5, 6mm) is assumed to be small when compared to the dimensions of the sample. The method of matched asymptotic expansions can be carried out with respect to d and allows deriving the mixed criterion [9]. The method consists in three steps. The first called "outer problem" considers the structure seen from a distance so that the cavity is no longer visible ($d \rightarrow 0$). The displacement field solution of the outer problem is written:

$$\underline{U}^d(x_1, x_2, l) = \underline{U}^0(x_1, x_2, 0) + \text{small correction} \quad (3)$$

where $\underline{U}^0(x_1, x_2, 0)$ is the solution to the unperturbed problem ($d=0$) and can be expanded in a Williams' series involving the T-stress term $r \underline{t}(\theta)$:

$$\underline{U}^0(x_1, x_2, l) = \underline{C} + \sigma_\infty r \underline{t}(\theta) \quad (4)$$

σ_∞ is the compressive remote load. (r, θ) is the polar system coordinates, and \underline{C} an irrelevant constant.

The second step is the inner problem. This step consists in being extremely close to the cavity: all variables are multiplied by $1/d$ and then $d \rightarrow 0$, the diameter of the cavity is set to 1. The displacement field solution of the inner problem is expanded in a classical asymptotic form:

$$\underline{U}^d(dy_1, dy_2, \mu) = F_0(d)\underline{V}^0(y_1, y_2, \mu) + F_1(d)\underline{V}^1(y_1, y_2, \mu) + \dots \quad (5)$$

where $F_1(d)/F_0(d) \rightarrow 0$ when $d \rightarrow 0$, $y_i = x_i/d$ and $\mu = l/d$.

In an intermediary zone, the two solutions (4) and (5) have to coincide. The displacement field solution of the actual problem is written:

$$\underline{U}^d(x_1, x_2, l) = \underline{U}^0(0,0,0) + \sigma_\infty d (\rho \underline{t}(\theta) + \hat{\underline{V}}^1(y_1, y_2, \mu)) \quad (6)$$

where $\underline{V}^1(y_1, y_2, \mu) = \rho \underline{t}(\theta) + \hat{\underline{V}}^1(y_1, y_2, \mu)$.

Once the displacement field is known, the stress and energy criteria can be derived. The stress criterion is:

$$\sigma_{11}(l) = \sigma_\infty \tilde{\sigma}_{11} \left(\hat{\underline{V}}^1 \left(0, \mu + \frac{1}{2}, 0 \right) \right) \geq \sigma_c \quad (7)$$

where $\tilde{\sigma}_{11} = d \sigma_{11}$. The energy criterion is:

$$\sigma_\infty^2 d \frac{A(\mu) - A(0)}{\mu} \geq G_c \quad (8)$$

$A(\mu)$ is a function depending only on the local properties of the material and the direction of the crack [9,10].

From (7) and (8), the equation giving the critical dimensionless length μ_0 at onset can be written:

$$\frac{1}{\tilde{\sigma}_{11} (\hat{\underline{V}}^1(0, \mu_0 + \frac{1}{2}, 0))^2} \frac{A(\mu_0) - A(0)}{\mu_0} = \frac{G_c}{d \sigma_c^2} \quad (9)$$

The loading at the initiation of the crack is:

$$\sigma_\infty = \frac{\sigma_c}{\tilde{\sigma}_{11} \left(\hat{\underline{V}}^1 \left(0, \mu_0 + \frac{1}{2}, 0 \right) \right)} \quad , \quad u_0 = \frac{(1-\nu)(1+\nu)}{E} \sigma_\infty \quad (10)$$

4 Results

The DIC shows that under compressive loading a pair of stable cracks emanate from the north and south poles of the cavity parallel to the loading direction. The theory predicts that these two cracks initiate from the hole at the same time and with the same length. In practice, it is not strictly the case. This can be explained by a lack of symmetry in the sample.

Figure 6 shows the displacement load predicted by the mixed criterion and the experimental displacement at the crack onset measured by DIC as functions of the diameter cavity.

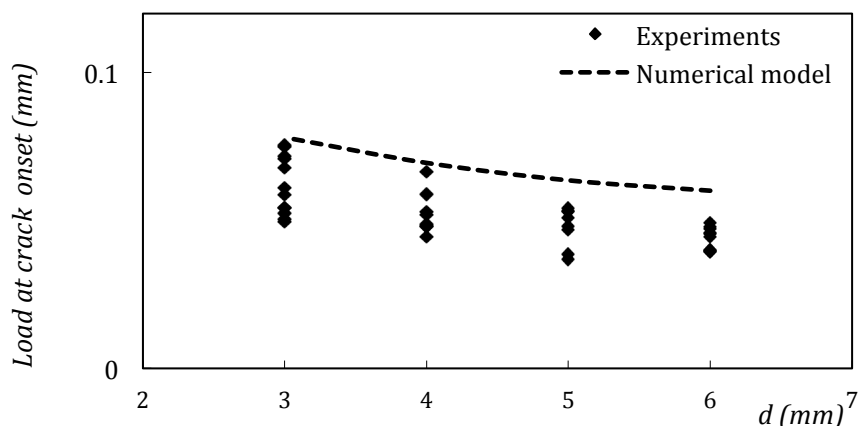


FIG. 6 – Crack onset: comparison between experiments and theory

Both theoretical model and experiments show that crack nucleation depends on the diameter of the cavity: the smaller the size of the cavity, the higher is the failure load. There is a size effect.

There is a rather good agreement between theory and experiments although not surprisingly the mixed criterion overestimates slightly experimental values. The model assumes a flawless specimen, whereas the slightest defect in the specimen can provoke the crack initiation earlier than expected. The fact that the pair of cracks does not nucleate exactly at the same time from the two poles results from the same effect: note that four samples have been tested for each diameter and that the loads at the onset of both the upper and lower cracks are reported. Moreover, the plaster is brittle: when drilling, some material is removed at the output of the drill bit on the backside of the sample.

5 Conclusion

In this work, the proposed method based on DIC proved to be a performing technique to detect the crack onset. The study confirmed that the model based on Leguillon's mixed criterion is in agreement with experiments: the load at crack onset depends on the diameter of the cavity: the smaller the cavity, the greater the load to initiate a crack. Further investigations will address multi-perforated specimens with the purpose of establishing improved models for porous materials.

References

- [1] Sammis C.G. and Ashby M.F., The failure of brittle porous solids under compressive stress states, *Acta Metall*, 34(3), 511-526, 1986.
- [2] Sutton M.A., Wolters W.J., Peters W.H., McNeill S.R., Determination of displacements using an improved digital correlation method, *Image Visual, Comput*, 1, 133-139, 1983.
- [3] Leguillon D., Strength or toughness? A criterion for crack onset at a notch, *European Journal of Mechanics A/Solids*, 21, 61-72, 2002.
- [4] Quesada D. and al, The role of the interbed thickness on the step-over fracture under overburden pressure, *Int J of Rock Mech Mining Sci*, 2008.
- [5] Chau K.T., Wei X.X., Wong R.H.C., Yu T.X., Fragmentation of brittle spheres under static and dynamic compressions: experiments and analyses, *Mechanics of Materials*, 32, 543-554, 2000.
- [6] Leguillon D., Sanchez-Palencia E., Computation of singular solutions in elliptic problems and elasticity, J. Wiley, New-york and Masson, Paris, 1987.
- [7] Picard D., Leguillon D., Putot C., A method to estimate the influence of the notch-root radius on the fracture toughness measurement of ceramics, *Journal of the European Ceramic Society*, 26, 1421-1427, 2006.
- [8] Dautriat J., Bornert M., and al, Localized deformation induced by heterogeneities in porous carbonate analysed by multi-scale digital image correlation, *Tectonophysics*, 503, 100-116, 2000.
- [9] Leguillon D., Quesada D., Putot D., Martin E., Prediction of crack initiation at blunt notches and cavities-size effects, *Engineering Fracture Mechanics*, 74, 2420-2436, 2007.
- [10] Yosibash Z., Priel E., Leguillon D., A failure criterion for brittle elastic materials under mixed-mode loading, *Int J Fract*, 141, 291-312, 2006.